Structure of electron waves at the (111) surface of a noble metal as a consequence of the topology of the Fermi surface: "quantum order" instead of "quantum chaos"

É. A. Pashitskiĭ
Institute of Physics, Ukrainian Academy of Sciences, 252650 Kiev, Ukraine

A. É. Pashitskiĭ
University of Wisconsin, Madison, WI 53706

(Submitted 20 May 1994)
Pis'ma Zh. Eksp. Teor. Fiz. **60**, No. 1, 35–41 (10 July 1994)

Standing electron waves with a period $d>15$ Å have been observed previously on (111) surfaces of single crystals of noble metals (Cu, Au, and Ag). These waves were observed by scanning tunneling microscopy. They were observed near adsorbed atoms (adatoms), near point defects (vacancies), and inside a "quantum corral" of 48 iron adatoms. It is shown here that these waves are not a consequence of a "quantum chaos" in a multiple scattering of electrons of 2D surface states by adatoms. These waves are instead a consequence of the topology of the Fermi surface of these metals. They arise as the result of the onset of a "quantum order," i.e., the formation of long-wave Friedel and Rudermann–Kittel oscillations in the course of Coulomb and exchange interactions of adatoms with 3D bulk states of the metal.

1. Several investigators have reported[1–3] observing standing electron waves of nanometer scale near isolated adatoms and point defects, near the edges of atomic steps, and also inside and outside an artificial "quantum corral" on the (111) faces of single crystals of noble metals (Cu, Au, and Ag). The observations were made by scanning tunneling microscopy. The corral, fabricated with the help of the tip of the scanning tunneling microscope, was a circular structure with a radius $R_0=71$ Å and consisted of 48 Fe adatoms on a Cu(111) surface. Large-scale waves of this sort, with a period $d>15$ Å, were attributed in Refs. 1–3 to an interference of electrons: incident electrons and electrons scattered by adatoms, occupying 2D surface states[4], with energies lying in one of the band gaps of the 3D bulk electron spectrum of the metal. The corresponding wave functions would be localized near the surface. On the other hand, a linear combination of square moduli of the one-electron wave functions (Bessel functions), which are the solutions of the 2D Schrödinger equation in a circular potential box with impenetrable walls, was used in Ref. 3 to describe the pattern of cylindrically symmetric standing waves inside a quantum corral. The concept of a "quantum chaos" was introduced in Ref. 5. This chaos would result from a multiple scattering of surface electrons by adatoms at the annular barrier of a quantum corral. However, the model of 2D surface states fails to explain such experimental results as the equality of the periods of the electron waves inside a quantum corral and on the free Cu(111) surface near isolated adatoms (defects),

the existence of sharp peaks in the electron density ("hard cores") at Fe adatoms, and the existence of deep dips ("craters") at the centers of "point defects."[1-3]

In this letter we show that all the features observed in the distribution of the electron density on (111) surfaces of noble metals can be explained in terms of Coulomb and exchange interactions of adatoms with bulk 3D electron states of these metals, along with the topology of the Fermi surfaces of these metals. Specifically, we mean the existence of open regions in ⟨111⟩ directions in the form of narrow "necks" of cylindrical symmetry on the nearly spherical Fermi surface. This circumstance promotes the onset of an ordered periodic structure of surface waves on (111) faces. These waves are long-wave Friedel oscillations[6] in a screened potential and in the distribution of the electron density around charged adatoms (defects)[7,8] and also Rudermann–Kittel oscillations in an indirect exchange interaction between adatoms via electrons of the metal.[9] For positively charged adatoms, the finite dipole moment leads to the onset of a sharp peak in the electron density (a "hard core"); for nearly neutral adatoms or negatively charged defects (vacancies), it leads to the existence of a deep dip ("crater") in the distribution of electrons on the surface of the metal, in agreement with the experimental data of Refs. 1–3.

2. We know[10] that the nearly spherical Fermi surface of noble metals (Cu, Au, and Ag) with a Fermi momentum $k_F = 1.36$ Å^{-1} has four pairs of diametrically positioned narrow necks of cylindrical symmetry along ⟨111⟩ crystallographic directions, which are perpendicular to (111) faces. The minimum radius of curvature (the Fermi momentum) at the intersection of a neck with the boundary of the Brillouin zone parallel to the (111) face of the crystal is $\tilde{k}_F \approx 0.21$ Å^{-1} for Cu (Ref. 11), $\tilde{k}_F \approx 0.19$ Å^{-1} for Au (Ref. 12), and $\tilde{k}_F \approx 0.14$ Å^{-1} for Ag (Ref. 13).

According to the theory worked out in Refs. 7–9, this situation means that ordered periodic structures of the electron density (the charge density) should arise on a (111) surface. These structures are spatial Friedel and Rudermann–Kittel oscillations. In addition to the short-wave Friedel and Rudermann–Kittel oscillations with a period $\pi/k_F \approx 2.3$ Å, which are determined by an interaction of adatoms with electrons on the nearly spherical part of the Fermi surface, and which decay rapidly with distance ($\propto R^{-3}$), there should be some far longer-wave Friedel and Rudermann–Kittel oscillations, corresponding to a contribution of electrons on the nearly cylindrical regions of the Fermi surface near the necks.[1)] These long-wave oscillations of the electron density are due to a square-root singularity in the static electron polarizability at the point $q_\parallel = 2\tilde{k}_F$ [$q_\parallel$ is the momentum transfer parallel to the (111) surface], because of the cylindrical symmetry of a pair of necks with respect to the [111] direction along the normal to the surface. The amplitude of these long-wave oscillations falls off with distance in proportion to R^{-2}, and the period is $d \approx 15$ Å for Cu, ≈ 16 Å for Au, and ≈ 22 Å for Ag, in good agreement with the experimental data of Refs. 1–3 for the periods of the electron waves.

It was observed in Refs. 1 and 2 that the period of the waves depends on the voltage applied to the tip of the scanning tunneling microscope. This dependence might be due to a variation along depth of the distribution of the electron density near the surface of the metal. Since the tunneling electrons are extracted from various depths in the metal (or injected to various depths) at different voltages, and since the Fermi momentum $\tilde{k}_F$ depends on the electron density, the periods of the Friedel and Rudermann–Kittel oscil-

lations acquire a voltage dependence which is not associated with a filling (or emptying) of 2D surface states.[4]

3. In addition to the circular cross section of one pair of necks, the cross sections of three other pairs of necks are projected at an angle $\varphi_0 = 70.5°$ onto the (111) hexagonal face (see the inset in Fig. 1a). Along each of the six symmetric directions, the projection of the Fermi momentum of one of the inclined pairs of necks is $\tilde{k}_F' = \tilde{k}_F \cdot \cos\varphi_0 = \tilde{k}_F/3$, while the projection of $\tilde{k}_F$ for the two other pairs of necks is $\tilde{k}_F'' = \tilde{k}_F \cdot \cos 30° = \tilde{k}_F\sqrt{3}/2$. This effect should give rise to a modulation of the axisymmetric Friedel and Rudermann–Kittel oscillations with a period $d = \pi/\tilde{k}_F$ both along the radius (with periods of $3d$ and $2d/\sqrt{3}$ along the symmetric directions) and along the azimuthal angle φ (with a period $\pi/3$). If we take the average over φ (from 0 to 2π) of this anisotropic structure of electron waves with a sixfold symmetry axis, we are left with a long-wave modulation of the fundamental Friedel and Rudermann–Kittel oscillations along the radius, with some average period[2)] $\bar{d} \approx 2d$.

On the other hand, the finite dipole moment of a charged adatom,[14,15] which exists because the center of the screening electron cloud in a semi-infinite metal does not coincide with the position of an adatom on the metal surface, leads to a monotonic dipole component in the screened Coulomb potential and in the distribution of the electron density, which decays as R^{-3} over distance.

The smoothed (average) profile of the perturbed electron density near a charged adatom (point defect) on the (111) surface of a noble metal can thus be approximated by the following simple expression (in terms of dimensionless variables), if we ignore the short-wave Friedel and Rudermann–Kittel oscillations corresponding to the spherical part of the Fermi surface (those oscillations fall off as R^{-3}):

$$\delta N_e(\rho) = \frac{\alpha}{(\rho+\rho_a)^3} + \frac{\beta_1\cos(\rho+\theta_1) + \beta_2\cos(\nu\rho+\theta_2)}{(\rho+\rho_a)^2} + f(\rho). \tag{1}$$

Here $\rho = 2\tilde{k}_F R$, $\rho_a = 2\tilde{k}_F r_a$, r_a is the radius of an adatom, α is the effective dipole–dipole interaction constant, β_1 and β_2 are the amplitudes of the fundamental component (with a period $d = \pi/\tilde{k}_F$) and of the modulating component (with a period $\bar{d} = d/\nu$) of the long-wave Friedel and Rudermann–Kittel oscillations, θ_1 and θ_2 are their phases, and $f(\rho)$ is a function which keeps the quantity $\delta N_e(\rho)$ positive regardless of the value of ρ, by virtue of the incompressibility of an electron Fermi liquid in a metal (because of electrical neutrality).

It follows from the condition $\delta N_e(\rho) > 0$ that $\delta N_e(\rho)$ can be represented as the square modulus of a multiparticle "coherent" wave function of screening electrons, $\Psi_e(\rho)$, which consists of a smoothly varying "dipole" part $\Psi_D(\rho)$ and an oscillating "Friedel" part $\Psi_F(\rho)$:

$$\delta N_e(\rho) \equiv |\Psi_e(\rho)|^2 = |\Psi_D(\rho) + \Psi_F(\rho)|^2. \tag{2}$$

If we assume that the functions $\Psi_D(\rho)$ and $\Psi_F(\rho)$ are real, then by comparing expressions (1) and (2) we find

$$\Psi_D(\rho) = \sqrt{\alpha}(\rho+\rho_a)^{-3/2}, \tag{3}$$

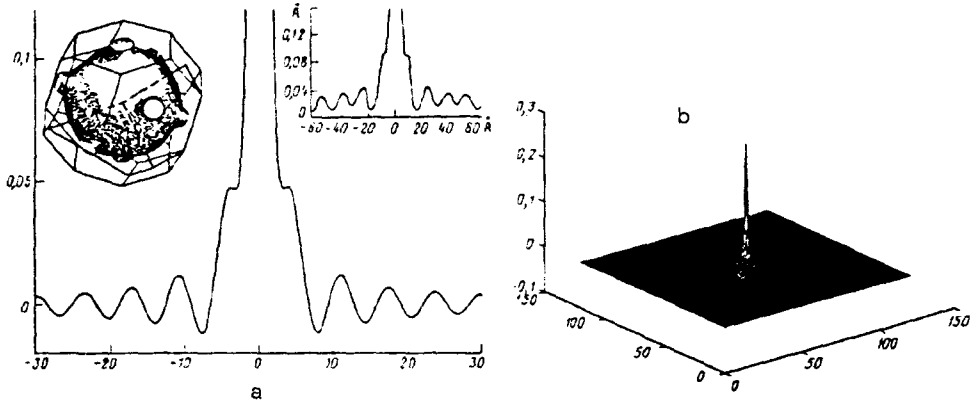

FIG. 1.

$$\Psi_F(\rho)=[\beta_1\cos(\rho+\theta_1)+\beta_2\cos(\nu\rho+\theta_2)]/2\sqrt{\alpha}(\rho+\rho_a)^{1/2}, \tag{4}$$

and we can treat the function $f(\rho)$ as the average (over the fundamental period d) of the square of the function $\Psi_F(\rho)$. We can use the approximation (we are ignoring long-wave "beats")

$$f(\rho)=\gamma(\rho+\rho_a)^{-1}. \tag{5}$$

The asymptotic behavior of $\Psi_F(\rho)$ at $\rho\gg\rho_a$ is essentially the same as that of Bessel functions ($\sim\rho^{-1/2}$).

4. Figures 1–3 show the results of numerical calculations from Eq. (1) with the help of (5). Figure 1a shows the central cross section of the profile of the electron density, $\delta N_e(\rho)$, for an Fe adatom with a radius $r_a=0.84$ Å (the Fe^{2+} ion) on the Cu(111) surface with $\bar{k}_F=0.21$ Å $^{-1}$, for the following parameter values: $a=2$, $\beta_1=0.3$, $\beta_2=0.1$, $\theta_1=\pi/4$, $\theta_2=3\pi/4$, $\rho_a=0.35$, $\gamma=0.02$, and $\nu=0.5$ (i.e., $\bar{d}=2d$). Shown at the upper right in this figure is the profile of the electron density observed in Ref. 3 by scanning tunneling microscopy. We see a complete qualitative agreement and a good quantitative agreement between (on the one hand) the theoretical results found on the basis of the multiparticle model of screening and an exchange interaction proposed here and (on the other) the experimental data. This agreement extends to the presence of a hard core (with a radius from 5 to 20 Å) in the distribution of the electron density around a charged Fe adatom.

The one-particle model of 2D surface states[3,4] can satisfactorily approximate only a periodic wave structure on a (111) surface; the presence of a hard core with a wide pedestal is simply postulated.

Figure 1b shows a 3D panoramic display of electron waves with a peak in the electron density at the center. This plot agrees well with the pattern of surface waves observed in Ref. 3 around an isolated Fe adatom.

Figure 2 shows a section of the electron density distribution for the following parameter values: $\alpha=-1$, $\beta_1=0.12$, $\beta_2=0.24$, $\theta_1=\theta_2=\pi/2$, $\rho_a=1$, $\gamma=0.02$, and $\nu=0.5$.

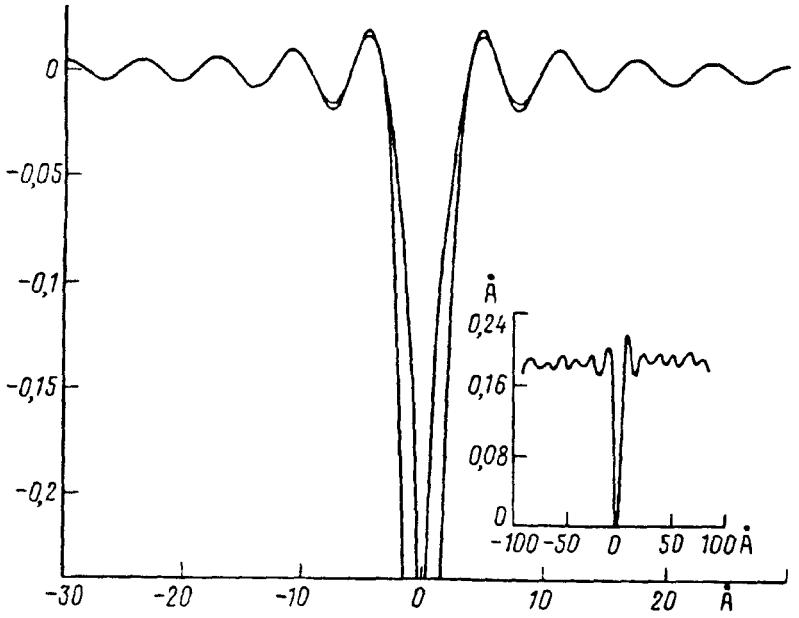

FIG. 2.

This figure corresponds to a negatively charged defect with a radius $r_a = 2.5$ Å, i.e., to a surface vacancy of a Cu^+ ion. Shown at the lower right in Fig. 2 is the distribution of the electron density near a point defect which was observed experimentally in Ref. 1 by scanning tunneling microscopy. This distribution agrees well with the calculated distribution. Neither the crater nor the hard core is described by the model of 2D surface states.

Figure 3 shows sections (a) and a panoramic display (b) of the electron density for

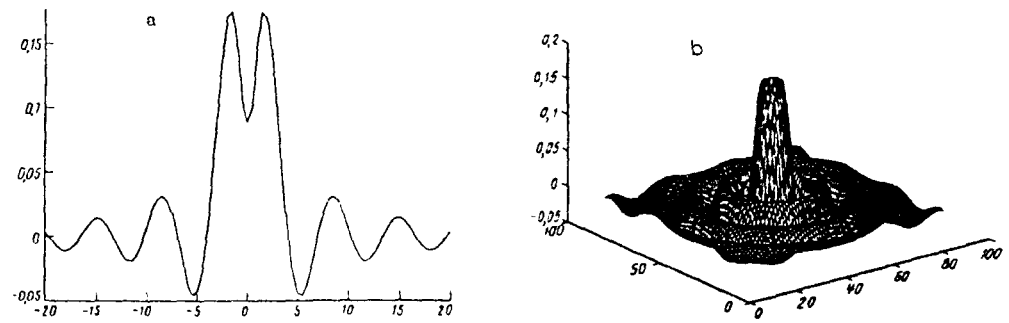

FIG. 3.

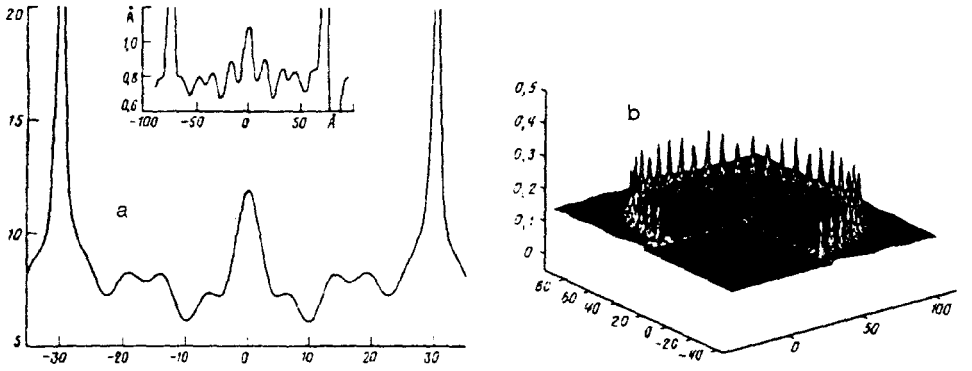

FIG. 4.

the parameter values $\alpha=0.2$, $\beta_1=0.06$, $\beta_2=0.12$, $\theta_1=\theta_2=4\pi/3$, $\rho_a=1.4$, $\gamma=0.02$, and $\nu=0.5$. These values correspond to a nearly neutral adatom of large radius ($r_a=3.3$ Å). An entity of this type, with a minimum in the electron density at the vertex (a "hill with a crater"), was observed near a quantum corral on a Cu(111) surface in Ref. 3.

5. The structure of the electron waves inside and around a quantum corral is the result of a superposition of the wave functions of individual Fe adatoms distributed uniformly on a circle of radius $R_0=71.3$ Å at the points with the coordinates[3)]

$$x_n=R_0\cos\varphi_n, \quad y_n=R_0\sin\varphi_n, \quad \varphi_n=n\pi/24. \tag{6}$$

The resultant electron density is determined by the square of the sum of the 48 wave functions $\Psi_e=\Psi_D+\Psi_F$ of the individual Fe adatoms:

$$\delta N_{48}(x,y)=\left\{\sum_{n=1}^{48}\left[\Psi_D(\rho_n(x,y))+\Psi_F(\rho_n(x,y))\right]\right\}^2, \tag{7}$$

where

$$\rho_n(x,y)=2\tilde{k}_F[(x-x_n)^2+(y-y_n)^2]^{1/2}. \tag{8}$$

Figure 4 shows results calculated from Eq. (7) with the help of (3), (4), (6), and (8). Part *a* shows a central section, and part *b* is an overall panoramic display of a quantum corral. The parameter values here are the same as in Fig. 1. We see that there is a completely satisfactory qualitative agreement between the theoretical results and the experimental wave profile shown in the inset in Fig. 4a.

The pattern of standing waves inside a quantum corral is thus not a consequence of a "quantum chaos" due to a multiple scattering of one-electron 2D states.[5] This pattern is instead the result of a superposition of "coherent" multielectron wave functions of Fe adatoms which are interacting with 3D states of the metal. In other words, it is a manifestation of a "quantum order" in a quantum corral.

We wish to thank A. G. Naumovets, Yu. G. Ptushinskiĭ, O. M. Braun, G. A. Katrich, and A. G. Fedorus for useful discussions of these results.

This study was supported by a grant from the Soros Foundation, awarded by the American Physical Society. The numerical calculations were carried out at the Applied Superconductivity Center of the University of Wisconsin, Madison, thanks to the cooperation and support of D. Larbalestier.

[1)]Like the de Haas–van Alphen oscillations with a large period in a magnetic field along the [111] direction.
[2)]This averaging occurs inside a quantum corral because of the different potentials of the Fe adatoms on a circle of radius R_0 (more on this below).
[3)]There is some scatter in the distances between neighboring adatoms (from 8.8 to 10.2 Å) in the actual structure of a quantum corral.[3] We are ignoring the scattering here. Rotations through an angle $\Delta\varphi = \pi/24$ result in an averaging of the anisotropic Friedel and Rudermann–Kittel oscillations over the angle φ.

[1] M. F. Grommie *et al.*, Nature **363**, 524 (1993).
[2] Y. Hasegawa and Ph. Avouris, Phys. Rev. Lett. **71**, 1071 (1993).
[3] M. F. Grommie *et al.*, Science **262**, 218 (1993).
[4] S. D. Kevan and R. H. Gaylord, Phys. Rev. B **36**, 5809 (1987).
[5] E. J. Heller *et al.*, Harvard Preprint, 1993.
[6] J. Friedel, Nuovo Cim. Suppl. **2**, 287 (1958).
[7] A. M. Gabovich and É. A. Pashitskiĭ, Fiz. Tverd. Tela (Leningrad) **18**, 377 (1976) [Sov. Phys. Solid State **18**, 220 (1976)].
[8] A. M. Gabovich *et al.*, Zh. Eksp. Teor. Fiz. **75**, 249 (1978) [Sov. Phys. JETP **48**, 124 (1978)]; Surface Sci. **94**, 179 (1980).
[9] K. H. Lau and W. Kohn, Surface Sci. **75**, 69 (1978).
[10] D. Shoenberg and D. J. Roaf, Roy. Soc. Phil. Trans. **255**, 85 (1962).
[11] B. Segall, Phys. Rev. **125**, 109 (1962).
[12] R. W. Morse *et al.*, J. Acoust. Soc. Am. **33**, 699 (1961).
[13] H. V. Bohm and V. J. Easterling, Phys. Rev. **125**, 605 (1962).
[14] L. A. Bol'shov *et al.*, Usp. Fiz. Nauk **122**, 125 (1977) [Sov. Phys. Usp. **20**, 432 (1977)].
[15] L. G. Il'chenko *et al.*, Fiz. Tverd. Tela (Leningrad) **22**, 2700 (1980) [Sov. Phys. Solid State **22**, 1576 (1980)]; Surface Sci. **121**, 375 (1982).

Translated by D. Parsons